

# Isobaric Yield Ratio Difference in Heavy-ion Collisions, and Comparison to Isoscaling

Chun-Wang MA<sup>1,\*</sup>, Shan-Shan WANG<sup>1</sup>, Yan-Li ZHANG<sup>1</sup>, and Hui-Ling WEI<sup>1</sup>

<sup>1</sup> *Department of Physics, Henan Normal University, Xinxiang 453007, China*

(Dated: June 23, 2021)

An isobaric yield ratio difference (IBD) method is proposed to study the ratio of the difference between the chemical potential of neutron and proton to temperature ( $\Delta\mu/T$ ) in heavy-ion collisions. The  $\Delta\mu/T$  determined by the IBD method (IB- $\Delta\mu/T$ ) is compared to the results of the isoscaling method (IS- $\Delta\mu/T$ ), which uses the isotopic or the isotonic yield ratio. Similar distributions of the IB- and IS- $\Delta\mu/T$  are found in the measured  $140A$  MeV  $^{40,48}\text{Ca} + ^9\text{Be}$  and the  $^{58,64}\text{Ni} + ^9\text{Be}$  reactions. The IB- and IS- $\Delta\mu/T$  both have a distribution with a plateau in the small mass fragments plus an increasing part in the fragments of relatively larger mass. The IB- and IS- $\Delta\mu/T$  plateaus show dependence on the  $n/p$  ratio of the projectile. It is suggested that the height of the plateau is decided by the difference between the neutron density ( $\rho_n$ ) and the proton density ( $\rho_p$ ) distributions of the projectiles, and the width shows the overlapping volume of the projectiles in which  $\rho_n$  and  $\rho_p$  change very little. The difference between the IB- and IS- $\Delta\mu/T$  is explained by the isoscaling parameters being constrained by the many isotopes and isotones, while the IBD method only uses the yields of two isobars. It is suggested that the IB- $\Delta\mu/T$  is more reasonable than the IS- $\Delta\mu/T$ , especially when the isotopic or isotonic ratio disobeys the isoscaling. As to the question whether the  $\Delta\mu/T$  depends on the density or the temperature, the density dependence is preferred since the low density can result in low temperature in the peripheral reactions.

PACS numbers: 25.70.Pq, 21.65.Cd, 25.70.Mn

## I. INTRODUCTION

In the models based on the free energy to predict the fragments in heavy-ion collisions (HICs) above the Fermi energy, the yield is mainly determined by the free energy, the chemical potential of proton and neutron, the temperature, etc. [1–4]. In the ratios between the fragment yields, some of the information which the fragment carries will cancel out, and the retained information is useful to study the properties of the colliding sources [2, 5], the fragment itself [6, 7], and the temperature of the reactions [1, 8]. The isoscaling method is one of the important methods to constrain the symmetry energy of the nuclear matter in HICs [2, 4, 9], which makes it important for the study of the nuclear equation of state [10]. The isoscaling phenomena are systemically studied experimentally, and extensively examined in theories from dynamical models to statistical models [5, 11–21]. The effects of the secondary decay, which significantly influence the results, are also investigated [13, 22–25]. Besides the isoscaling method, the isobaric yield ratio is promoted to determine the symmetry energy of the fragments produced in HICs in a modified Fisher model [6, 26–29]. At the same time, the isotopic ratio and the isobaric ratio are also used to study the temperatures of the colliding sources [1, 30–37] or the heavy fragments in HICs [8, 37, 38]. Since both the isoscaling method and the isobaric ratio method are deduced in the framework of the free energy theories, and they both relate the yield of fragments to the symmetry energies of the colliding sources, it is important to compare the nuclear symmetry energy determined by them.

In this article, the difference between the chemical potentials of the neutron and proton will be compared using the isoscaling method and the isobaric ratio method. In Sec. II, the isoscaling and the isobaric ratio difference methods will be deduced in the framework of the grand-canonical ensembles. In Sec. III, the fragment yields in the  $140A$  MeV  $^{40,48}\text{Ca} + ^9\text{Be}$  and  $^{58,64}\text{Ni} + ^9\text{Be}$  reactions will be analyzed using the isoscaling method and the isobaric yield ratio (IYR) method, and the results will be compared. A summary will be presented in Sec. IV.

## II. MODEL DESCRIPTION

The isoscaling and the isobaric ratio difference (IBD) methods in the grand-canonical ensembles will be introduced briefly. In the grand-canonical limit, the yield of a fragment with mass  $A$  and neutron-excess  $I$  ( $I = N - Z$ ) is given by [39, 40]

$$Y(A, I) = CA^\tau \exp\{[F(A, I) + \mu_n N + \mu_p Z]/T\}, \quad (1)$$

where  $C$  is a constant.  $N$  and  $Z$  are the neutron and proton numbers.  $\tau$  is nonuniform in different reaction systems [41].  $\mu_n$  and  $\mu_p$  are chemical potentials of the neutron and proton, respectively;  $F(A, I)$  is the free energy of the cluster (fragment), and  $T$  is the temperature.

The isoscaling method is as follows: for one fragment in two reactions of the same measurements, based on Eq. (1), the yield ratio of the two reactions,  $R_{21}^{IS}(N, Z)$ , can be defined as [2, 3]

$$R_{21}^{IS}(N, Z) = Y_2(N, Z)/Y_1(N, Z) = C' \exp(\alpha N + \beta Z), \quad (2)$$

where  $C'$  is an overall normalization constant which originates from the different reaction systems.  $\mu_n$  and  $\mu_p$

\* Email: machunwang@126.com

are assumed to change very slowly;  $\alpha = \Delta\mu_n/T$  with  $\Delta\mu_n = \mu_{n2} - \mu_{n1}$ , and  $\beta = \Delta\mu_p/T$  with  $\Delta\mu_p = \mu_{p2} - \mu_{p1}$ , which reflect the properties of the colliding sources. In the isotopic ratios,  $\beta$  cancels out and  $\alpha$  can be fitted; and in the isotonic ratios,  $\alpha$  cancels out and  $\beta$  can be fitted.  $\alpha \approx -\beta$  is found, and  $\alpha$  can be related to the symmetry energy ( $C_{sym}$ ) in nuclear mass of the colliding source by  $\alpha = 4\frac{C_{sym}}{T}[(\frac{Z_1}{A_1})^2 - (\frac{Z_2}{A_2})^2]$ , or some similar relationships [9, 14, 15, 17].

The isobaric yield ratio (IYR) is used to study the symmetry energy of the fragment at finite temperatures [6, 8, 27–29]. When using IYR to study the  $\mu_n$  and  $\mu_p$ , the analysis method should be reconstructed. Starting from Eq. (1), in one single reaction, the IYR between the isobars differing by 2 units in  $I$ ,  $R^{IB}(I+2, I, A)$ , can be defined as

$$R^{IB}(I+2, I, A) = Y(A, I+2)/Y(A, I) \\ = \exp\{[F(I+2, A) - F(I, A) + \mu_n - \mu_p]/T\}, \quad (3)$$

The  $CA^\tau$  term in Eq. (1) cancels out and the system dependence is removed. Assuming that the isobars in the ratio have the same temperature, only the retained  $\mu_n$  and  $\mu_p$  are related to the colliding sources. Taking the logarithm of Eq. (3), one can obtain,

$$\ln R^{IB}(I+2, I, A) = (\Delta F + \Delta\mu)/T, \quad (4)$$

where  $\Delta F = F(I+2, A) - F(I, A)$ , and  $\Delta\mu = \mu_n - \mu_p$ . In two reactions of the same measurements, the difference between the IYRs, i.e. the IBD method, can be defined as,

$$\Delta \ln R_{21}^{IB} = \ln[R_2^{IB}(I+2, I, A)] - \ln[R_1^{IB}(I+2, I, A)] \\ = \Delta\mu_n/T - \Delta\mu_p/T = \Delta\mu/T = \alpha - \beta, \quad (5)$$

Eq. (5) also shows the relationship between the results of the isoscaling parameters ( $\alpha$  and  $\beta$ ) and the IBD method. For convenience, the IBD and isoscaling  $\Delta\mu/T$  are labeled as IB- $\Delta\mu/T$  ( $\equiv \Delta \ln R_{21}^{IB}$ ) and IS- $\Delta\mu/T$  ( $\equiv \alpha - \beta$ ), respectively.

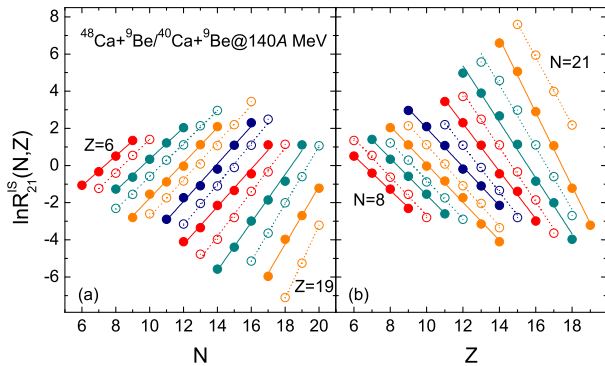


FIG. 1. (Color online) (a) The isotopic yield ratio of the isotopes from  $Z = 6$  to 19, and (b) the isotonic yield ratio of the isotones from  $N = 8$  to 21 in the 140A MeV  $^{40,48}\text{Ca} + ^9\text{Be}$  reactions [42]. The lines are the linear fitting results.

### III. RESULTS AND DISCUSSIONS

The yields of the fragments produced in the 140A MeV  $^{40,48}\text{Ca} + ^9\text{Be}$  and the  $^{58,64}\text{Ni} + ^9\text{Be}$  reactions were measured by Mocko *et al.* at the National Superconducting Cyclotron Laboratory (NSCL) in Michigan State University. The details of the measurements were described in Ref. [42]. The isoscaling phenomena in these reactions were studied in Ref. [13], and the isotopic (isotonic) yield distributions in these reactions were studied in Ref. [43]. In this article, the IB- and the IS- $\Delta\mu/T$  associated with the fragments in these reactions will be analyzed. The analysis will be performed between the isotopic  $^{48}\text{Ca}/^{40}\text{Ca}$  and  $^{64}\text{Ni}/^{58}\text{Ni}$  reactions, the  $n/p$  symmetric  $^{58}\text{Ni}/^{40}\text{Ca}$  reactions, and the neutron-rich  $^{48}\text{Ca}/^{64}\text{Ni}$  reactions. The reaction of the relatively small  $n/p$  projectile is denoted as 1, and the other one as 2. The isoscaling parameters  $\alpha$  and  $\beta$  are obtained from the linear fitting of the isotopic ratio and the isotonic ratio in the chosen reactions according to Eq. (2). For example, in Fig. 1, the isoscaling phenomena of the fragments in the 140A MeV  $^{40,48}\text{Ca} + ^9\text{Be}$  reactions are shown. In Figs. 1(a) and (b), the isotopic scaling and the isotonic scaling are plotted, respectively (similar results can be found in Ref. [13]).  $\alpha$  ( $\beta$ ) equal to the slope of the linear fitting of the isotopic (isotonic) scaling. For one fragment, the IS- $\Delta\mu/T$  is calculated using the  $\alpha$  and  $\beta$  obtained from its  $Z$  isotopes and  $N$  isotones, respectively. For IB- $\Delta\mu/T$ , the IYR in each reaction is calculated first, then the difference between the IYRs in the two reactions is calculated according to Eq. (5).

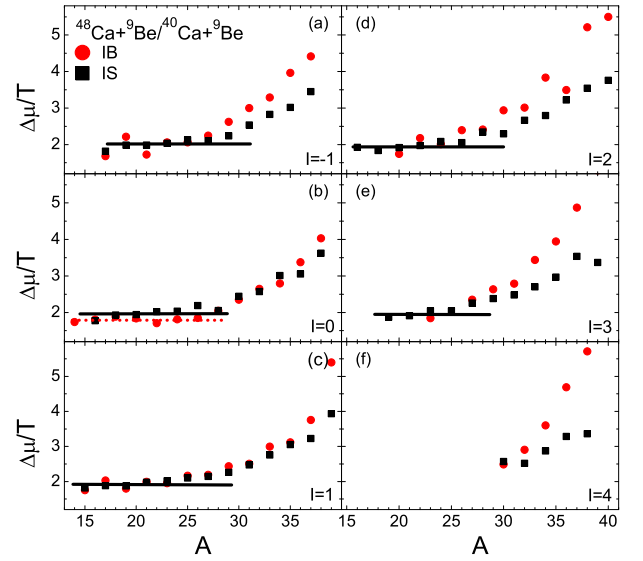


FIG. 2. (Color online) The IB- and IS- $\Delta\mu/T$  in the 140A MeV  $^{40,48}\text{Ca} + ^9\text{Be}$  reactions [42].  $I = N - Z$  is the neutron-excess. The lines are for guiding the eyes to the plateaus.

In Fig. 2, the IB- and IS- $\Delta\mu/T$  in the  $^{48}\text{Ca}/^{40}\text{Ca} + ^9\text{Be}$  reactions are plotted. Very similar trends of the IB- and IS- $\Delta\mu/T$  distributions in each  $I$ -chain of fragments

are found. In each  $I$ -chain, both the IB- and IS- $\Delta\mu/T$  in the small- $A$  fragments form plateaus (around  $\Delta\mu/T = 2$ ), and  $\Delta\mu/T$  increases as  $A$  increases in the large- $A$  fragments. The plateaus of the IB- and IS- $\Delta\mu/T$  almost overlap, and it is interesting that the IB- and IS- $\Delta\mu/T$  have very little difference in the  $I = 0$  [panel (b)] and the  $I = 1$  [panel (c)] fragments. Except for the  $I = 0$  and  $I = 1$  fragments, differences between the IB- and IS- $\Delta\mu/T$  in the large- $A$  fragments are shown.

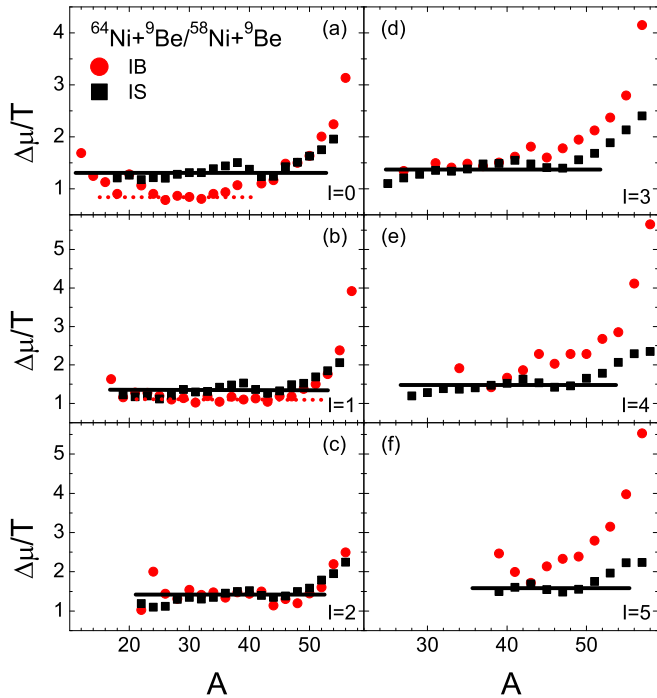


FIG. 3. (Color online) The IB- and IS- $\Delta\mu/T$  in the 140 MeV  $^{58,64}\text{Ni} + ^9\text{Be}$  reactions [42]. The lines are for guiding the eyes to the plateaus.

In Fig. 3, the IB- and IS- $\Delta\mu/T$  in the  $^{64}\text{Ni}/^{58}\text{Ni} + ^9\text{Be}$  reactions are plotted. Very similar results as the  $^{48}\text{Ca}/^{40}\text{Ca}$  reactions are found, except that the values of the plateaus decrease to about 1.4. The values of the IB- and IS- $\Delta\mu/T$  almost overlap in the  $I = 1$  [panel (b)] and the  $I = 2$  [panel (c)] fragments. The  $n/p$  for  $^{48}\text{Ca}/^{40}\text{Ca}$  is 1.4/1.0, which is larger than the value 1.286/1.071 for  $^{64}\text{Ni}/^{58}\text{Ni}$ . Comparing to the results in the  $^{48}\text{Ca}/^{40}\text{Ca}$  reactions, obviously larger widths of the IB- and IS- $\Delta\mu/T$  plateaus in the  $^{64}\text{Ni}/^{58}\text{Ni}$  reactions are found.

From the results shown in Figs. 2 and 3, for the plateau, its height (the value) and its width (the nuclei range it covers) should be noticed. In the statistical models [43, 44], the yield of a fragment to some extent is decided by the density distributions of protons ( $\rho_p$ ) and neutrons ( $\rho_n$ ) of the projectile and the target nuclei. A nucleus can be assumed to have a core region, in which  $\rho_p$  and  $\rho_n$  change very little, and a skirt region, in which  $\rho_p$  and  $\rho_n$  change fast. The  $\rho_p$  distributions of isotopes can be assumed to be similar, especially when the masses of the isotopes do not differ much. This indicates that,

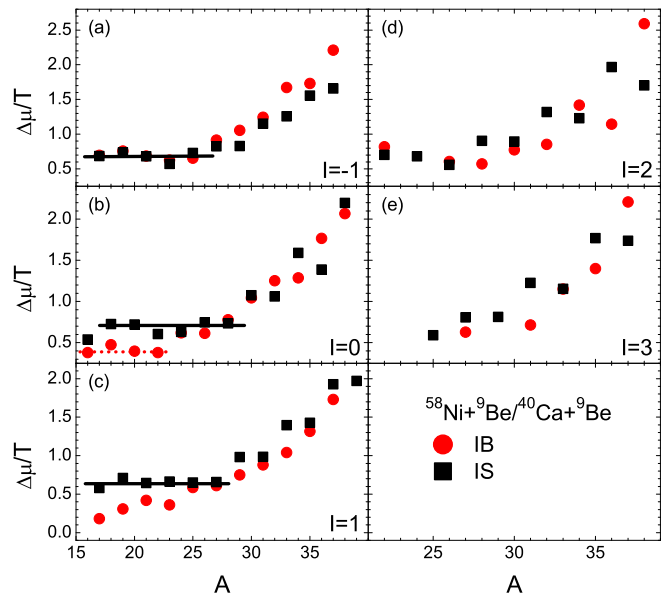


FIG. 4. (Color online) The IB- and IS- $\Delta\mu/T$  in the 140 MeV  $^{40}\text{Ca} + ^9\text{Be}$  and  $^{58}\text{Ni} + ^9\text{Be}$  reactions [42]. The lines are just for guiding the eyes of the plateaus.

the height of the plateau is decided by the difference between  $\rho_n$  and  $\rho_p$  in the projectiles, and the width shows the overlapping volume of the projectiles in which  $\rho_n$  and  $\rho_p$  vary slowly. Regarding the  $\Delta\mu/T$  in the isotopic projectile reactions, the height of the plateau indicates the difference between the  $\rho_n$  distributions of the projectiles.

In addition to the similarity of the isotopic distributions in the  $^{40}\text{Ca}/^{48}\text{Ca}$  and the  $^{58}\text{Ni}/^{64}\text{Ni}$  reactions, the similarity of the isotopic and the isotonic distributions in the  $^{58}\text{Ni}/^{40}\text{Ca}$  and the  $^{48}\text{Ca}/^{64}\text{Ni}$  reactions were also investigated in Refs. [43, 45]. It is found that the isotopic or isotonic yield distribution shows dependence on  $\rho_n$  and  $\rho_p$  of the projectiles. In the isoscaling method, the system effects do influence  $\alpha$  and  $\beta$ . In the IBD method, the system effects are also removed in the IYR. Thus the  $\Delta\mu/T$  in the  $n/p$  symmetric  $^{58}\text{Ni}/^{40}\text{Ca}$  reactions, and the neutron-rich  $^{48}\text{Ca}/^{64}\text{Ni}$  reactions can also be analyzed. In Fig. 4, the  $\Delta\mu/T$  in the  $^{58}\text{Ni}/^{40}\text{Ca}$  reactions are plotted. The  $n/p$  of  $^{58}\text{Ni}/^{40}\text{Ca}$  is 1.071/1.0, thus  $\rho_n$  and  $\rho_p$  for them can be assumed to have similar trends but differ in values. In Fig. 4, very small differences between the IB- and IS- $\Delta\mu/T$  are found in each  $I$ -chain. The values of the plateaus decrease to about 0.7, and in the  $I = 0$  and 1 chain, the IB-plateaus become even smaller.

The IB- and IS- $\Delta\mu/T$  in the  $^{48}\text{Ca}/^{64}\text{Ni}$  reactions are plotted in Fig. 5. The  $n/p$  ratio of  $^{48}\text{Ca}/^{64}\text{Ni}$  is 1.4/1.286. Though large differences between the IB- and IS- $\Delta\mu/T$  in the  $I \leq 2$  fragments are shown, similar values of the IB- and IS- $\Delta\mu/T$  in the  $I \geq 3$  ( $A \geq 25$ ) fragments are found. The plateaus in the  $I \leq 3$  chains decrease to smaller than 0.5. The characteristics of the IB- and IS- $\Delta\mu/T$  distributions are very similar to those of the isotopic or isotonic distributions shown in Ref. [43], i.e.,

the density dependence of  $\rho_n$  and  $\rho_p$  in the projectiles.

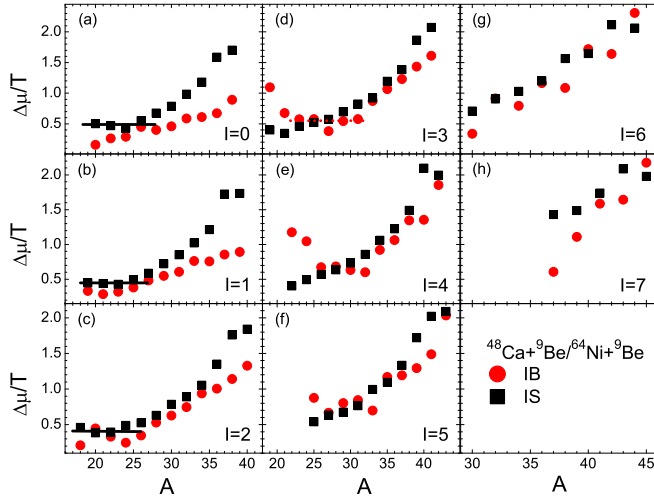


FIG. 5. (Color online) The IB- and IS- $\Delta\mu/T$  in the 140A MeV  $^{48}\text{Ca} + ^9\text{Be}$  and  $^{64}\text{Ni} + ^9\text{Be}$  reactions [42]. The lines are for guiding the eyes to the plateaus.

In Fig. 2-5, similarities between IB- and IS- $\Delta\mu/T$  are shown, i.e., the plateaus and the values in the small- $A$  fragments of the  $^{48}\text{Ca}/^{40}\text{Ca}$  and  $^{64}\text{Ni}/^{58}\text{Ni}$  reactions, most fragments of the  $^{58}\text{Ni}/^{40}\text{Ca}$ , and large- $A$  fragments of the  $^{48}\text{Ca}/^{64}\text{Ni}$  reactions; while the differences between the IB- and IS- $\Delta\mu/T$  are shown in the large- $A$  fragments of the  $^{48}\text{Ca}/^{40}\text{Ca}$  and  $^{64}\text{Ni}/^{58}\text{Ni}$  reactions. The values of the plateaus show a dependence of the  $n/p$  ratio of the reaction systems, which are about 2, 1.4, 0.7, and 0.5 in the  $^{48}\text{Ca}/^{40}\text{Ca}$ ,  $^{64}\text{Ni}/^{58}\text{Ni}$ ,  $^{58}\text{Ni}/^{40}\text{Ca}$ , and  $^{48}\text{Ca}/^{64}\text{Ni}$  reactions.

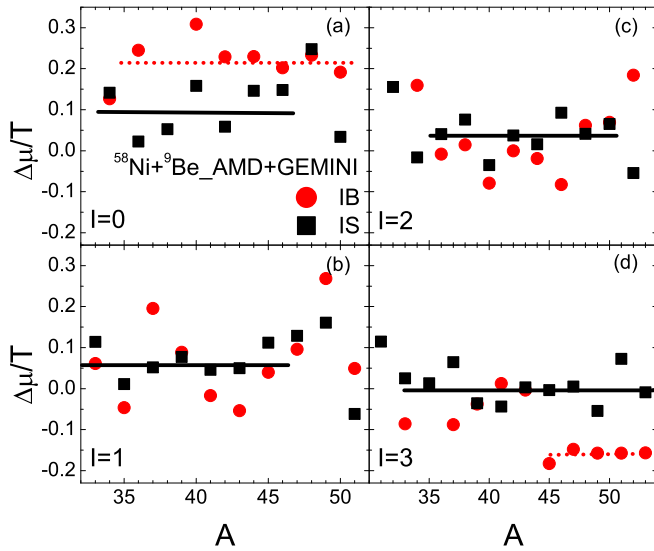


FIG. 6. (Color online) The IB- and IS- $\Delta\mu/T$  between the fragments in the impact parameter regions of R1 ( $b=0-2$  fm) and R2 ( $b=6-8$  fm) in the 140A MeV  $^{58}\text{Ni} + ^9\text{Be}$  reactions calculated using the AMD + GEMINI models.

To see more clearly on this point, we performed a simulation of the 140A MeV  $^{58}\text{Ni} + ^9\text{Be}$  reaction using a microscopic transport model. Though there are many choices—such as the quantum molecular dynamics (QMD and its improved versions) models [21, 22, 34, 47–49], the AMD model [15, 16, 51, 52], and different methods to form the cluster or fragment [50, 53]—the AMD model plus the sequential decay GEMINI code [53] have been used to simulate the reaction, since similar works are performed, and the experimental yields of fragments are well reproduced [46]. In the calculation, the standard Gogny interaction (Gogny-g0) is used [54], the fragments are formed using a coalescence radius,  $R_c = 5$  fm in the phase space at the time  $t = 500$  fm/c in AMD. Two cuts of impact parameters are used in the fragments analysis, i.e.,  $b=0-2$  fm (labeled as R1) and  $b=6-8$  fm (labeled as R2). The results are plotted in Fig. 6. Since  $^{58}\text{Ni}$  is a symmetric nucleus, its  $\rho_n$  and  $\rho_p$  distributions are very similar, and the densities only decrease sharply in the very edge of the nucleus. In R1 and R2, the difference between  $\rho_n$  and  $\rho_p$  is also very small. According to the assumption that the plateau of  $\Delta\mu/T$  depends on  $n/p$  of the projectiles, the plateaus of the IB- $\Delta\mu/T$  should be very small. In Fig. 6, it can be seen that the IB- and IS- $\Delta\mu/T$  are very similar, and their values are very small. The IS- $\Delta\mu/T$  of most fragments are in a range of  $0.1 \pm 0.1$ , and the IB- $\Delta\mu/T$  of the  $I = 0 - 2$  chains are  $0 \pm 0.1$ . This indicates that the IB- and the IS- $\Delta\mu/T$  have very little difference when  $\rho_n$  and  $\rho_p$  of the two projectiles are similar, and differ if  $\rho_n$  and  $\rho_p$  of the two projectiles are different.

Furthermore, the difference between the IB- and IS- $\Delta\mu/T$  should also be discussed. Generally, the IB- and IS- $\Delta\mu/T$  should be the same since they are obtained from the same fragments and in the same theory. Though in most fragments the IB- and IS- $\Delta\mu/T$  are very similar, the difference between the IB- and IS- $\Delta\mu/T$  are also shown in many fragments. For examples, in fragments where the IB- and IS- $\Delta\mu/T$  are different, the IB- $\Delta\mu/T$  are larger than the IS- $\Delta\mu/T$  in the  $^{48}\text{Ca}/^{40}\text{Ca}$  and  $^{64}\text{Ni}/^{58}\text{Ni}$  reactions, while the IB- $\Delta\mu/T$  are smaller than the IS- $\Delta\mu/T$  in the  $^{58}\text{Ni}/^{40}\text{Ca}$  and  $^{48}\text{Ca}/^{64}\text{Ni}$  reactions. According to Eq. (2), the isoscaling parameters  $\alpha$  ( $\beta$ ) are obtained from the linear correlation between the isotopic (isotonic) ratio and neutron (proton) numbers, and  $\alpha$  ( $\beta$ ) is the same for all the isotopes (isotones). In other words,  $\alpha$  ( $\beta$ ) is the scaled parameter for all the isotopes (isotones). For one fragment, its  $\alpha$  ( $\beta$ ) is constrained by its isotopes (isotones), thus  $\alpha$  ( $\beta$ ) can not reflect the difference between the isotopes or isotones. While according to Eq. (5), the IB- $\Delta\mu/T$  result only relies on the two related isobars, and the difference between isobars of different masses can be obviously shown. It is suggested that since the IBD method uses only two isobars, the IB- $\Delta\mu/T$  result is not influenced by the rest fragments, and more precise results than the isoscaling method can be obtained, especially when the fragment disobeys the isoscaling.

Finally, we discuss the temperature effect in the  $\Delta\mu/T$ .  $\mu_n$  and  $\mu_p$  depend on both the density and the temperature. In theories based on the free energy, it is difficult to separate the free energy and the temperature [6, 27]. In the IB- and the IS- $\Delta\mu/T$ , it is also difficult to separate  $\Delta\mu$  and  $T$ . Besides the density effects in  $\Delta\mu/T$ , the temperature also influences  $\Delta\mu/T$ . Actually, the temperature should be defined at thermal equilibrium, but in intermediate energy HICs no thermal equilibrium is reached. In other words, the temperature is nonuniform in the collisions. In QMD, the "temperature" can be extended to the non-equilibrium situations and extracted in the local density approximation [55]. In grand-canonical ensemble theory, the temperature is supposed to be the same, but differs in each reaction system. In a recent work using a canonical thermodynamic model, a temperature profile of impact parameter ( $b$ ) is introduced, in which the temperature decreases as  $b$  increases [56]. Considering the multiple sources collisions of different strengths according to the impact parameters, the temperature changes with the excitation energy. In the Fermi-gas relationship the correlation between the excitation energy per nucleon ( $E^*/A$ ) and temperature is  $E^*/A = T^2/a$ , or  $T = \sqrt{E^*a/A}$ , in which  $a = Ak$  and  $k$  is the inverse level density parameter. In Ref. [13], in the  $^{48}\text{Ca}/^{40}\text{Ca} + ^9\text{Be}$  reactions,  $\alpha$  is found to decrease when  $E^*/A$  increases (which corresponds to  $T = 1.2 - 2.14$  MeV), but  $\alpha$  tends to be similar if  $E^*/A$  is high. Noting that  $\alpha \approx -\beta$ , the temperature dependence of  $\alpha$  can also explain the plateau plus the increasing part of the IB- and IS- $\Delta\mu/T$  distributions as follows: if  $\Delta\mu$  are uniform in the source, the plateau forms in the fragments which have high  $E^*/A$ , while the  $\Delta\mu/T$  increases when  $E^*/A$  decreases in the fragments which have low  $E^*/A$ . In the statistical abrasion-ablation (SAA) model, the excitation energy is  $E^* = 13.3\Delta A$  MeV, in which  $\Delta A$  is the number of nucleons removed from the projectile by the ablation-abrasion process [8, 43]. Then  $T = \sqrt{13.3k\Delta A/A}$ . In peripheral collisions, due to the low density of nucleons, the abraded nucleons are fewer than those in the central collisions, which results in the relative low temperature. To some extent, the low temperature is a result of the low density in the peripheral collisions, which is similar to the temperature profile in Ref. [56]. Thus low density can also result in an increase of  $\Delta\mu/T$ . In an isobaric method, the temperature of the measured heavy fragment is suggested to be similar due to the significant influence of the secondary decay process [8]. Thus, though the density dependence and the temperature dependence

of  $\Delta\mu/T$  cannot be totally separated, the density dependence is preferred since the low temperature is one result of the low density.

#### IV. SUMMARY

To summarize, in the article, a new IBD method is proposed to investigate  $\Delta\mu/T$  of the colliding sources, and the result is compared with the result of the usually used isoscaling method within the same grand-canonical model. The IB- and IS- $\Delta\mu/T$  are found to be similar in the distributions, which both have a plateau in small mass fragments plus an increasing part in relatively larger mass fragments. The IB- and IS- $\Delta\mu/T$  plateaus show dependence on the  $n/p$  ratio of the projectiles. It is suggested that the height of the plateau is decided by the difference between  $\rho_n$  and  $\rho_p$  in the projectiles, and the width shows the overlapping volume of the projectiles in which  $\rho_n$  and  $\rho_p$  change very little. The difference between the IB- and IS- $\Delta\mu/T$  is explained by  $\alpha$  and  $\beta$  being constrained by the many isotopes and isotones, while the IBD method only uses the yields of two isobars. It is suggested that the IB- $\Delta\mu/T$  is more reasonable than the IS- $\Delta\mu/T$ , especially when the isotopic or isotonic ratio disobeys the scaling. As to the question whether  $\Delta\mu/T$  depends on the density or the temperature of the colliding, the density dependence is preferred since the low density can result in the low temperature in the peripheral reactions.

#### ACKNOWLEDGMENTS

This work is supported by the National Natural Science Foundation of China under Contract No. 10905017, the Program for Science&Technology Innovation Talents in Universities of Henan Province (HASTIT), and the Young Teacher Project in Henan Normal University (HNU), China. We also thank the helpful guides of Dr. HUANG Mei-Rong at the Institute of Modern Physics (IMP), Chinese Academy of Sciences, for the AMD simulation and data analysis. A useful discussion with Professor Roy Wada at IMP is also acknowledged. The AMD simulation is performed on the high-performance computing center at the College of Physics and Electrical Engineering, HNU.

---

[1] S. Albergo *et al.*, Nuovo Cimento A **89**, 1 (1985).  
 [2] Y. G. Ma *et al.*, Phys. Rev. C **69**, 064610 (2004); Phys. Rev. C **72**, 064603 (2005).  
 [3] H. S. Xu *et al.*, Phys. Rev. Lett. **85**, 716 (2000).  
 [4] A. S. Botvina *et al.*, Phys. Rev. C **65**, 044610 (2002).  
 [5] M. B. Tsang *et al.*, Phys. Rev. Lett. **86**, 5023 (2001).

[6] M. Huang *et al.*, Phys. Rev. C **81**, 044620 (2010).  
 [7] A. S. Hirsch *et al.*, Phys. Rev. C **29**, 508 (1984).  
 [8] C. W. Ma *et al.*, Phys. Rev. C **86**, 054611 (2012).  
 [9] M. Colonna, Phys. Rev. Lett. **110**, 042701 (2013).  
 [10] B.-A. Li *et al.*, Phys. Rep. **464**, 113 (2008).  
 [11] M. Huang *et al.*, Nucl. Phys. A **847**, 233 (2011).

- [12] D. Q. Fang *et al.*, J. Phys. G: Nucl. Part. Phys. **34**, 2173 (2007).
- [13] Y. Fu *et al.*, Chin. Phys. Lett. **26**, 082503 (2009).
- [14] Z. Chen *et al.*, Phys. Rev. C **81**, 064613 (2010).
- [15] A. Ono *et al.*, Phys. Rev. C **68**, 051601(R) (2003).
- [16] A. Ono *et al.*, Phys. Rev. C **70**, 041604(R) (2004).
- [17] S. R. Souza *et al.*, Phys. Rev. C **80**, 044606 (2009).
- [18] G. A. Souliotis *et al.*, Phys. Rev. C **68**, 024605 (2003).
- [19] G. A. Souliotis *et al.*, Phys. Rev. C **73**, 024606 (2006).
- [20] C. O. Dorso, Phys. Rev. C **73**, 034605 (2006).
- [21] W. D. Tian *et al.*, Chin. Phys. Lett. **22**, 306 (2005).
- [22] P. Zhou *et al.*, Phys. Rev. C **84**, 037605 (2011).
- [23] M. B. Tsang *et al.*, Phys. Rev. C **64**, 054615 (2001).
- [24] T. X. Liu *et al.*, Phys. Rev. C **69**, 014603 (2004).
- [25] M. Colonna *et al.*, Eur. Phys. J. A **30**, 165 (2006).
- [26] C. W. Ma *et al.*, Chin. Phys. Lett. **29**, 092101 (2012).
- [27] C. W. Ma *et al.*, Phys. Rev. C **83**, 064620 (2011).
- [28] Chun-Wang Ma *et al.*, Eur. Phys. J. A **48**, 78 (2012).
- [29] C.-W. Ma *et al.*, Chin. Phys. Lett. **29**, 062101 (2012); Chin. Phys. C **37**, 024102 (2013).
- [30] A. L. Goodman *et al.*, Phys. Rev. C **30**, 851 (1984).
- [31] Y. G. Ma *et al.*, Phys. Rev. C **60**, 024607 (1999).
- [32] Y. G. Ma *et al.*, Phys. Rev. C **71**, 054606 (2005).
- [33] J. B. Natowitz *et al.*, Phys. Rev. C **52**, R2322 (1995).
- [34] J. Su and F. S. Zhang, Phys. Rev. C **84**, 037601 (2011); J. Su, *et al.*, Phys. Rev. C **85**, 017604 (2012).
- [35] J. Wang *et al.*, Phys. Rev. C **72**, 024603 (2005).
- [36] R. Wada *et al.*, Phys. Rev. C **55**, 227 (1997).
- [37] W. Trautmann *et al.* (ALADIN Collaboration), Phys. Rev. C **76**, 064606 (2007).
- [38] C. W. Ma, *et al.*, Commun. Theo. Phys. **59**, 95 (2013).
- [39] C. B. Das *et al.*, Phys. Rev. C **64**, 044608 (2001).
- [40] M. B. Tsang *et al.*, Phys. Rev. C **76**, 041302(R) (2007).
- [41] M. Huang *et al.*, Phys. Rev. C **82**, 054602(R) (2010).
- [42] M. Mocko *et al.*, Phys. Rev. C **74**, 054612 (2006).
- [43] C. W. Ma *et al.*, Phys. Rev. C **79**, 034606 (2009).
- [44] C.-W. Ma *et al.*, Phys. Rev. C **82**, 057602 (2010).
- [45] C. W. Ma *et al.*, Chin. Phys. B **18**, 4781 (2009).
- [46] M. Mocko *et al.*, Phys. Rev. C **78**, 024612 (2008).
- [47] S. Kumar *et al.*, Phys. Rev. C **81**, 014611 (2010); S. Gautam *et al.*, J. Phys. G: Nucl. Part. Phys. **37**, 085102 (2010); S. Gautam *et al.*, Phys. Rev. C **83**, 014603 (2011); *ibid.*, Phys. Rev. C **83**, 034606 (2011).
- [48] N. Wang, Z. Li, and Z. Wu, Phys. Rev. C **65**, 064608 (2002); Y. Zhang and Z. Li, Phys. Rev. C **71**, 024604 (2005); *ibid.*, Phys. Rev. C **74**, 014602 (2006); Y. Zhang *et al.*, Phys. Lett. B **664**, 145 (2008).
- [49] S. Kumar *et al.*, Phys. Rev. C **84**, 044620 (2011); S. Kumar *et al.*, Phys. Rev. C **86**, 044616 (2012).
- [50] S. Goyal and R. K. Puri, Phys. Rev. C **83**, 047601 (2011); Y. K. Vermani *et al.*, J. Phys. G: Nucl. Part. Phys. **37**, 015105 (2010); R. K. Puri, and J. Aichelin, J. Comp. Phys. **162**, 245(2000).
- [51] A. Ono and H. Horiuchi, Phys. Rev. C **53**, 2958 (1996).
- [52] A. Ono, Phys. Rev. C **59**, 853 (1999).
- [53] R. J. Charity *et al.*, Nucl. Phys. A **483**, 371 (1988).
- [54] J. Dechargé and D. Gogny, Phys. Rev. C **21**, 1568 (1980).
- [55] R. K. Puri *et al.*, Nucl. Phys. A **575**, 733 (1994).
- [56] S. Mallik *et al.*, Phys. Rev. C **84**, 054612 (2011).